AIR FLOW MODEL FOR SUB-SLAB DEPRESSURIZATION SYSTEMS DESIGN

Thierno M.Oury Diallo[1,2], Bernard Collignan[1], Francis Allard[2]

1 CSTB Health Division,
84 avenue Jean-Jaurès
77447 Marne-la-Vallée, France

2 University of La Rochelle-
(LaSIE, FRE-CNRS 3474)
Avenue Michel Crépeau
17042 La Rochelle, France
**Corresponding author:thierno.diallo@cstb.fr*

ABSTRACT

Soil gas pollutants (Radon, VOCs, etc...) entering buildings are known to pose serious health risks to building's occupants, and various systems have been developed to lower this risk. Soil Depressurization Systems (SDS) are among the most efficient mitigation systems protecting buildings against soil pollutants. Two kinds of SDS are currently used: active and passive systems. Active systems are mainly use fans, which enables the mechanical sub-slab's air extraction. Passive systems use natural thermal forces and wind effect to extract air from the sub-slab. Until now, no airflow model effective enough has been developed to help design those systems. In this paper, a novel method, based on analytical models of soil gas transfer, is presented to design Soil Depressurization Systems. The developed air flow models take into account various kinds of substructures: slab-on-grade and basement (supported slab and floating slab). These airflow models are integrated in a multizone airflow and heat transfer building code. This integration takes into account various parameters such as meteorological conditions (stack effect, wind), building characteristics (e.g. building envelope, airtightness…) and ventilation systems. Preliminary field verification results for extracted flow using passive sub-slab depressurization in an experimental house are presented and discussed. The results obtained show that, depending on local meteorological conditions and building characteristics, the airflow model is accurate enough, and represents a useful SDS design tool.

KEYWORDS

Soil gas, passive sub-slab depressurisation, active sub-slab depressurisation, airflow model, design.

1 INTRODUCTION

Radon migration from subsurface soil to indoor air can represents a major health risk, as it increases the risk of lung-cancer. The most effective system preventing soil gas pollutants entering buildings is the Soil Depressurisation System (SDS). It prevents the convective transfer of the soil gas pollutant towards the building (USEPA, 1993; Collignan and O'Kelly, 2003; Collignan et al., 2004). This system is generally equipped with an exhaust fan which maintains a constant depressurisation beneath the building. It is sometimes mentioned that this depressurisation could be obtained naturally using natural buoyancy and wind effect. The advantages of this system include lower operation and maintenance costs. The ability and the efficiency of this technique have not yet been assessed properly, and need to be tested. In the literature, some analytical (Reddy et al., 1991; Cripps, 1998) and numerical (Gadjil et al., 1991; Bonnefous, 1992; Halford and Freeman, 1992) models have been developed to characterize such systems. Reddy et al. (1991) used an analytical airflow SDS model based on the exponential non-Darcy flow. As explained by Gadjil et al. (Gadjil et al., 1991), this model has a certain limit, since it is assumed that there are no cracks in building's slab, and that the interface between the sub slab gravel and the soil is impermeable. In fact, the presence of crack in building slab can have a significant impact on the pressure field and velocity in the gravel layer. According to experiments of Turk (Turk, 1991), 40-90% of the air drawn in by the SDS comes from inside of the building. The Reddy et al. model is only valid when soil

permeability is higher than gravel permeability by a considerable margin. This model cannot be used when the soil is proven permeable. Cripps (Cripps, 1998) has developed also an analytical model based on the Darcy-Forchheimer equation. Counter to Reddy et al. model, this model includes a peripheral crack of the slab. However, it considers the soil impermeable just like the Reddy et al. model. Gadjil et al. (Gadjil et al., 1991) and Bonnefous (Bonnefous, 1992) used a 3 D finite element model to study the performance of SDS systems. This model takes into account the diffusive and convective transport in the soil and sub slab gravel. However, the transport (convection and diffusion) within the slab is ignored. It considers the airflow through the peripheral crack of the slab. Despite its assumptions, this model allows the identification of mechanisms and factors contributing to the performance of SDS systems. To study the effectiveness of passive SDS in reducing radon entry rate in building, Harold and Freeman (Harold and Freeman, 1996) used the finite element model Rn3D, which simulates the convective and diffusive transport in a porous medium. Transport in the porous medium is governed by Fick's law of diffusion and Darcy's law of convection. This model considers both the building slab permeability and the peripheral crack of the slab. Compared to numerical models, analytical models are more attractive in terms of use by professionals, even if they represent fewer of the phenomenon involved. A one year monitoring of a passive Soil Depressurisation System has been undertaken in an experimental dwelling on the CSTB site (Abdelouhab et al., 2010; Collignan et al, 2008). The ongoing mechanical efficiency of the whole system was recorded. Those experimental results show the potential advantage of passive SDS for protecting buildings against the soil gas pollutants. Its efficiency, however, depends on meteorological conditions and buildings characteristics.

In this context, it appeared necessary to have a tool for the design of such a system, which may take into account these different parameters. Such a tool could enable testing of the availability of passive SDS in a specific context and helps with its design. In this paper, an analytical model developed to characterise mechanical running of passive and active SDS is presented. Compared with the existing SDS analytical airflow models, this model considers the permeability of the soil, witch affects the effectiveness of the SDS. It assumes the permeability of the slab, and the existence of the slab's peripheral crack. The airflow in the subslab gravel layer is governed by the Darcy-Forchehimer equation. Two slab substructures are considered: the floating slab and the supported slab. This model is coupled with a ventilation model and enables the verification of passive SDS functionning, during a year, for given specific meteorological conditions and building characteristics. Results obtained have been compared with experimental results and some sensitivity studies were presented.

2 PRESENTATION OF PREVIOUS EXPERIMENTAL STUDY

A one year monitoring of a passive Soil Depressurisation System had been undertaken in an experimental dwelling on CSTB site. The objective of this study was to assess the mechanical efficiency of such a system during a year. This experiment and the main results obtained are summarized below (Abdelouhab et al., 2010; Collignan et al., 2008). During its construction, an SDS has been installed into the experimental dwelling. For the purpose of this experiment, it had been conceived to be monitored in a passive way. To analyse the performance of such a system during time, the air velocity in the duct and the air temperature at the entrance of the duct were measured each minute with a probe. The indoor temperature in following analyses is the average temperature measured in different rooms. Likewise, basement depressurization has been measured between the gravel layer and indoor environment at floor level with a differential manometer. Wind (velocity and direction) and external temperature have been recorded from a weather station located close to the experimental dwelling (figure 1 a)

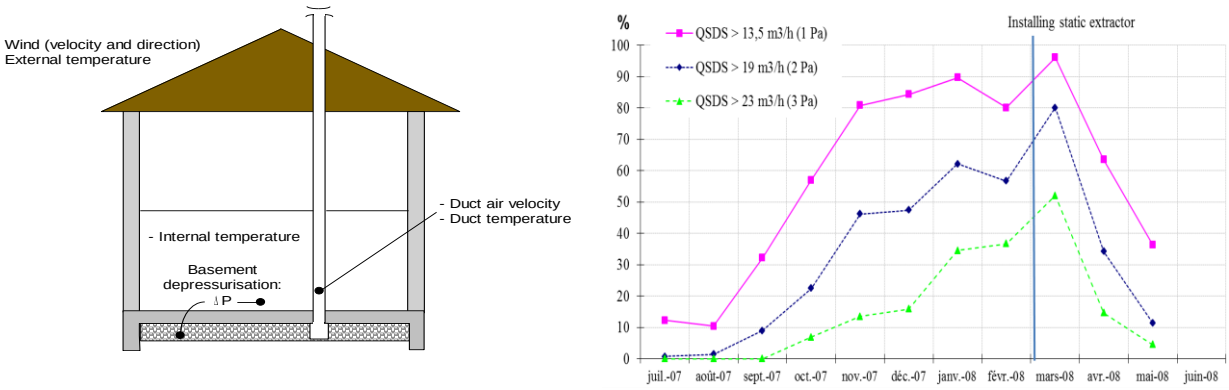

a b

Figure 1: a) Parameters measured during the one year follow up b) Percentage of running time of the system along year above three thresholds.

Results obtained consist of an important database of the physical variables measured each minute during the year. One of the main results obtained during this experiment is presented in figure 1 b. It shows the percentage of running time of the system during the year above three thresholds of extracted air flow rates from the basement. These experimental results showed the advantage of passive SDS, on the one hand to protect the building against the soil gas pollutants. On the other hand, this technique works at a marginal cost, unlike mechanical SDS. It appears also that natural running of SDS is highly variable during the year. However, in these experiments, percentage of running time could be significant and mainly during the winter season. This is an interesting result because a preventive solution is mainly needed during this period to block soil gas pollutants entrance due to convective fluxes between ground and inhabited volume. A secondary result showed the advantage of installing an efficient static extractor at the exit of the duct to ameliorate the running of the system. As a conclusion, it could be said, that efficient running of passive SDS depends on weather conditions and some building and environmental parameters. So that, it appears interesting to develop a model that can assess performance of such a system in specific conditions. This model could help to design the passive SDS.

3 DEVELOPMENT OF ANALYTICAL AIR FLOW MODEL

An analytical model has been developed to determine the mechanical running characteristics of a passive SDS (air flow and depressurization) as a function of building characteristics and meteorological conditions (wind and temperature difference). The conceptual model to quantify airflow through porous media is based on an analogy between the heat transfer conduction and the air flow as presented in previous works (Diallo et al. 2012). Airflow through porous media follows generally Darcy law except in gravel layer where Darcy-Forchheimer law is used. Air flow through passive SDS duct is due to pressure difference between gravel layer and the environment. It can come from indoors and from the soil:

$$Q_{SDS} = Q_{ind} + Q_{soil} \quad (1)$$

Q_{SDS}, Q_{ind} and Q_{soil} (in m^3/s) are respectively air flow into the duct, from indoors and from the soil respectively. Figure 2 shows a scheme of passive SDS integrated in its environment

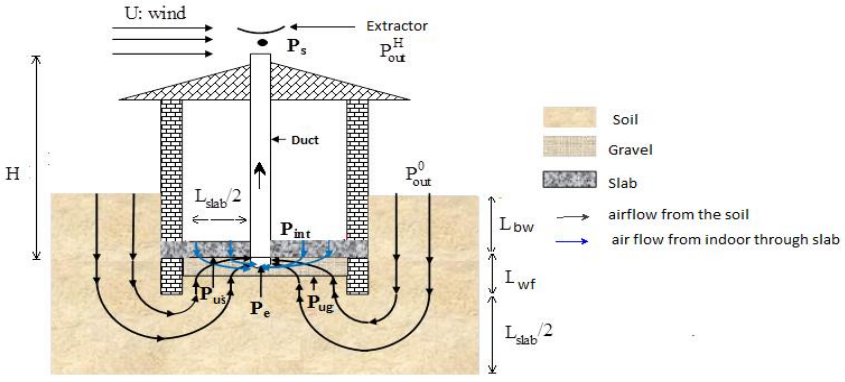

a

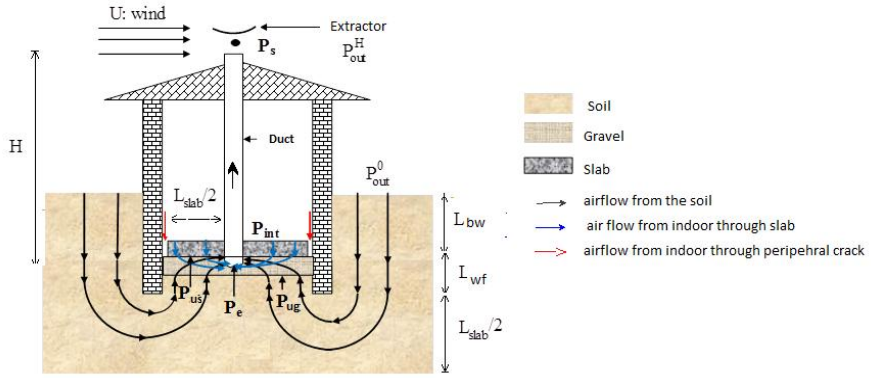

b

Figure 2: SDS integrated in a dwelling, with different pressures to be considered: a) supported slab substructure b) floating slab substructure.

3.1 Determination of air flow from indoors (Q_{IND}) for supported slab (figure 2 a)

Pressure loss between indoors and duct entrance can be written as follows:

$$P_{ind} - P_e = (P_{ind} - P_{US}) + (P_{US} - P_e) \quad (2)$$

with P_{ind} being the pressure above the floor, P_e the pressure at duct entrance and P_{US} the pressure under the slab, in Pa. Pressure loss between indoors and under slab can be expressed as:

$$(P_{ind} - P_{US}) = R_{slab} \times Q_{ind} \quad (3)$$

with (Diallo et al., 2012):

$$R_{slab} = \frac{e_{slab} \times \mu}{k_{slab} \times S_{slab}} \quad (4)$$

with e_{slab} (m) being the thickness of the slab, μ (Pa.s) the dynamic viscosity of air, k_{slab} (m²) the air permeability of slab and S_{slab}(m²) the surface of the slab.

Based on expressions presented in Annex for the determination of pressure loss in gravel between two surfaces, pressure loss between under slab and duct entrance is as followed:

$$P_{US} - P_e = R_{g1} c A_h^{-1} Q_{ind}^2 + R_{g1} Q_{ind} \quad (5)$$

with c the Forchheimer coefficient, R_{g1} (Pa/m^3/s) the gravel resistance between under slab and duct entrance and A_h (m²) the surface of the hemisphere at the entrance of the duct. Replacing eq. (3) and eq. (5) in eq. (2), we obtain:

$$\left(\frac{R_{g1} c}{A_h}\right) Q_{ind}^2 + (R_{g1} + R_{slab}) Q_{ind} - (P_{ind} - P_e) = 0 \quad (6)$$

Solving eq. (6) with positive discriminant, air flow from indoors can be expressed:

$$Q_{ind}=\left[-\left(R_{g1}+R_{slab}\right)+\left[\left(R_{g1}+R_{slab}\right)^2+4\left(\frac{R_{g1}c}{A_h}\right)(P_{ind}-P_e)\right]^{0.5}\right]\left[2\left(\frac{R_{g1}c}{A_h}\right)\right]^{-1} \quad (7)$$

3.2 Determination of air flow from indoors (Q_{IND}) for floating slab (figure 2 b)

To determine the air flow indoors for floating slab, the resistance of the slab R_{slab} in eq. (7) is just replaced by the total resistance R_{tot} of the slab and the peripheral crack which are in parallel.

$$Q_{ind}=\left[-\left(R_{g1}+R_{tot}\right)+\left[\left(R_{g1}+R_{tot}\right)^2+4\left(\frac{R_{g1}c}{A_h}\right)(P_{ind}-P_e)\right]^{0.5}\right]\left[2\left(\frac{R_{g1}c}{A_h}\right)\right]^{-1} \quad (8)$$

The total resistance R_{tot} is:

$$R_T=\left[R_{crack}^{-1}+R_{slab}^{-1}\right]^{-1} \quad (9)$$

The resistance of the slab R_{slab} is given by eq.4 and the resistance of the crack is:

$$R_{crack}=\frac{12\times e_{slab}\times\mu}{d^3 P} \quad (10)$$

With d (m) being the width crack, P (m) the perimeter of the slab.

3.3 Determination of air flow from the soil (Q_{SOIL})

Pressure loss between outdoors and duct entrance can be written as followed:

$$P_{out}^0-P_e=\left(P_{out}^0-P_{ug}\right)+\left(P_{ug}-P_e\right) \quad (11)$$

with P_{out}^0 and P_{ug} being the outdoor pressure at ground level and the pressure under gravel layer respectively, in Pa. Pressure loss between outdoors and under slab can be expressed:

$$\left(P_{out}^0-P_{ug}\right)=R_{soil}\times Q_{soil} \quad (12)$$

with (Diallo et al. 2012):

$$R_{soil}=\left[\frac{k_{soil}P}{\pi\mu}\ln\left(\frac{1+\left(\frac{\pi}{2L_{wf}+L_{bw}}\right)\left(\frac{L_{slab}+e_m}{2}\right)}{1+\left(\frac{\pi}{L_{wf}+L_{bw}}\right)\left(\frac{e_m}{2}\right)}\right)\right]^{-1} \quad (13)$$

with k_{soil} (m²) the air permeability of the soil, P (m) the perimeter of the slab, L_{wf} (m) the length of foundation, L_{slab} (m) the length of the slab and e_m (m) the thickness of the foundation wall. L_{bw} (m) is the basement wall height. If L_{bw}=0 in eq., we get slab-on-grade substructure. Based on expressions presented in Annex for the determination of pressure loss in gravel between two surfaces, pressure loss between under gravel and duct entrance is as followed:

$$P_{ug}-P_e=R_{g2}cA_{duct}^{-1}Q_{soil}^2+R_{g2}Q_{soil} \quad (14)$$

with R_{g2} (Pa/m^3/s) the gravel resistance between under gravel and duct entrance and A_{duct} (m²) the surface of the cylinder at the entrance of the duct. Replacing eq. (12) and eq. (14) in eq. (11), we obtain:

$$\left(\frac{R_{g2}c}{A_{duct}}\right)Q_{soil}^2+\left(R_{g2}+R_{soil}\right)Q_{soil}-(P_{out}^0-P_e)=0 \quad (15)$$

Solving eq. (15) with positive discriminant, air flow from the soil can be expressed:

$$Q_{soil}=\left[-\left(R_{g2}+R_{soil}\right)+\left[\left(R_{g2}+R_{soil}\right)^2+4\left(\frac{R_{g2}c}{A_{duct}}\right)(P_{out}^0-P_e)\right]^{0.5}\right]\left[2\left(\frac{R_{g2}c}{A_{duct}}\right)\right]^{-1} \quad (16)$$

Replacing eq. (16) and eq. (7) in eq. (1), air flow into the duct for supported slab can be deduced:

$$Q_{SDS} = \left[-\left(R_{g1} + R_{slab}\right) + \left[\left(R_{g1} + R_{slab}\right)^2 + 4\left(\frac{R_{g1}\,c}{A_h}\right)(P_{ind} - P_e) \right]^{0.5} \right] \left[2\left(\frac{R_{g1}\,c}{A_h}\right) \right]^{-1} + \left[-\left(R_{g2} + R_{soil}\right) + \left[\left(R_{g2} + R_{soil}\right)^2 + 4\left(\frac{R_{g2}\,c}{A_{duct}}\right)(P^0_{out} - P_e) \right]^{0.5} \right] \left[2\left(\frac{R_{g2}\,c}{A_{duct}}\right) \right]^{-1} \quad (17)$$

By replacing R_{slab} by R_{tot} in eq. 17, air flow into the duct for floating slab is deducted.

3.3.1. Determination of pressure difference into the duct

This pressure difference is the result of the equilibrium between pressure losses and stack effect. It can be expressed as:

$$(P_e - P_s) = \Delta P_{friction} + \Delta P_{singularity} + \Delta P_{stack} \quad (18)$$

with pressure losses due to friction into the duct and due to singularity, respectively:

$$\Delta P_{friction} = \lambda \frac{H}{D_H} \times \frac{1}{2}\rho\left(\frac{Q_{SDS}}{A_{duct}}\right)^2 \; ; \; \Delta P_{singularity} = \sum \zeta_i \times \frac{1}{2}\rho\left(\frac{Q_{SDS}}{A_{duct}}\right)^2$$

with λ and ξ_i are the linear and singular pressure loss coefficients respectively (I.E. IDEL'CIK, 1969). D_H (m) is the hydraulic diameter of the duct, ρ (kg/m^3) the volumic mass of the air and h (m) the height of the duct. The stack effect into the duct ΔP_{Stack} is:

$$\Delta P_{stack} = (\rho_e - \rho_s) g H \quad (19)$$

with ρ_e and ρ_s(kg/m^3) the densities of the air at the entrance and at the exit of the duct respectively. It is assumed that T_e and ρ_e are known. The unknown is:

$$\rho_s = \rho_e T_e / T_s \quad (20)$$

To determine T_s and based on enthalpy balance into the duct, temperature along the duct for a given height (h) can be written (Mounajed, 1989):

$$T(h) = T_{int} + (T_e - T_{int})\exp(-\omega \alpha_m h), \text{ with: } \omega = \frac{\pi D}{\rho Q_{SDS} C_p} \quad (21)$$

In eq. (21), T_{int} is supposed to be known. α_m is a global exchange coefficient between indoors and air flow into the duct. It could be determined considering three resistances in parallel as followed:

$$\frac{1}{\alpha_m S_{int}} = \frac{1}{S_{int} h_{int}} + \frac{\ln(r_1 / r_2)}{2\pi\lambda H} + \frac{1}{h_{ext} S_{ext}} \quad (22)$$

With S_{int} (m²) and S_{ext} (m²) the internal and external surface of the duct respectively, r_1 (m) and r_2 (m) the internal and external radius of the duct respectively. h_{int} and h_{ext} are classical heat exchange coefficients for natural convection that can be found in Elenbass (1942). Eq. (21) enables to determine T(H) (= T_s). Once T_s determined, as a function of Q_{SDS}, we can write ρ_s as a function of Q_{SDS} with eq. (20) and as a function of P_{ind}, P_e and P^0_{out} using eq. (17).

3.3.2. Determination of pressure loss at the exit of the duct (static extractor)

In presence of wind, shape of the extractor diminishes outdoor pressure at the exit of the duct and we have:

$$P_s - P^H_{out} = \frac{1}{2}\rho C_{p,out} U^2 \quad (23)$$

with P^H_{out} the outdoor pressure at the exit duct level in Pa, $C_{p,out}$ a suction coefficient depending on the shape of the extractor and U (m/s) wind velocity.

3.3.3. Determination of pressure loss at the exit of the duct (mechanical extractor)

The depression created by a mechanical extractor can be expressed by a quadratic law (Mounajed, 1989):

$$\Delta P_{ext} = \frac{\rho}{\rho_0}\left(P_x + C_x Q_{sds}^2\right) \quad (24)$$

Where Px and Cx are coefficients from the overall characteristic of the extractor used. ρ and ρ_0 are respectively the reference density of air at 20 ° C and the actual density. This depression can also be obtained by polynomial from the fan characteristic used (Koffi, 2009) regression. This type of extractor is not used in this study; this extractor model is presented just to show that the SDS model developed can be adapted for this type of extractor. In this study we focused on the passive extractor because the experiments are conducted with this type of extractor.

3.3.4. Determination of Q_{SDS}

Using eq. (18) to eq. (23), pressure difference between the entrance of the duct and outdoors can be written:

$$(P_e - P_{out}^H) = (P_e - P_S) + (P_S - P_{out}^H) = \left(\lambda\frac{L}{D_H} + \sum_1 \zeta_i\right) \times \frac{1}{2}\rho\left(\frac{Q_{SDS}}{A_{duct}}\right)^2 - (\rho_s - \rho_e)gH + \frac{1}{2}\rho C_{p,out} U^2 \quad (25)$$

From eq. (20), air flow into the duct can be deduced:

$$Q_{SDS} = A_{duct}\left(2\left[(P_e - P_{out}^H) + (\rho_e - \rho_s)gH - \frac{1}{2}\rho C_{p,out} U^2\right]\left[\rho\left(\lambda\frac{L}{D_H} + \sum\zeta_i\right)\right]^{-1}\right)^{0.5} \quad (26)$$

Using the two expressions of Q_{SDS} (eqs. (17) and (26)), we can write:

$$\begin{aligned}
&\left[-(R_{g1} + R_{slab}) + \left[(R_{g1} + R_{slab})^2 + 4\left(\frac{R_{g1}c}{A_h}\right)(P_{ind} - P_e)\right]^{0.5}\right]\left[2\left(\frac{R_{g1}c}{A_h}\right)\right]^{-1} \\
&+\left[-(R_{g2} + R_{soil}) + \left[(R_{g2} + R_{soil})^2 + 4\left(\frac{R_{g2}c}{A_{duct}}\right)(P_{out}^0 - P_e)\right]^{0.5}\right]\left[2\left(\frac{R_{g2}c}{A_{duct}}\right)\right]^{-1} \\
&-A_{duct}\left(2\left[(P_e - P_{out}^H) + (\rho_e - \rho_s)gH - \frac{1}{2}\rho C_{p,out} U^2\right]\left[\rho\left(\lambda\frac{L}{D_H} + \sum\zeta_i\right)\right]^{-1}\right)^{0.5} = 0
\end{aligned} \quad (27)$$

In this equation, if P_{ind}, P_{out}^0 and P_{out}^H are known. As explained previously in §3.3.1, ρ_s can be expressed as a function of P_{ind}, P_e and P_{out}^0. The only unknown is P_e. Once P_e is calculated, Q_{SDS} can also be calculated for given conditions.

3.4 Integration in a ventilation model

For this study a numerical ventilation model developed under Mathlab-Simulink environment has been used (Koffi, 2009). Equation (27) can be integrated. This equation can be solved using Newton method. For a given time step, P_{ind}, P_{out}^0 and P_{out}^H are given by ventilation model. P_e, Q_{SDS}, Q_{soil} and Q_{ind} are calculated. Determination of Q_{ind} could modify indoor mass balance, so it is needed to have a loop on mass balance of ventilation model; to obtain a converged result.

This integration allows us to obtain mechanical running characteristics of a passive SDS all along the year for given environmental conditions (meteorology) and building characteristics (dimensions, ventilation system, air permeability). It makes it possible to conduct relevant studies on given parameters to test the ability of passive SDS to run in given conditions and to dimension it.

4 RESULTS

4.1 Confrontation with experimental results

Passive SDS model presented in § 2 has been compared to results of the experiment presented in § 1. For this confrontation, it was needed to have additional data as soil and slab permeabilities. For slab permeability, value obtained during complementary experiments using tracer gas (Abdelouhab, 2011) is used. For soil permeability and thanks to a collaboration with IRSN (IRSN, 2012), soil permeability had been assessed. It had appeared that soil permeability around the experimental dwelling was relatively heterogeneous and some averages were necessary to be used in our model. Figure 3 presents a confrontation of experimental and numerical results obtained for air flow through passive SDS and for gravel depressurization between July 2007 and February 2008 in the experiment.

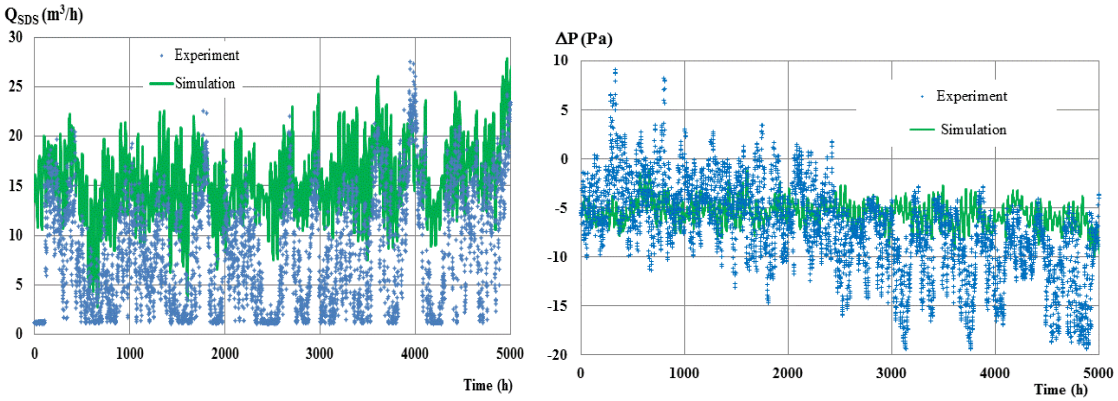

(a) (b)

Figure 3: comparison between experimental and numerical for air flow through passive SDS (a) and gravel depressurization (b) between July 2007 and February 2008.

Based on these results, it can be said that numerical results obtained with our model are relevant. However, it is observed that experimental results are more variable than numerical ones. Also, there is generally an overestimation of the air flow through the SDS duct with calculations, which implies an underestimation of depressurization in the gravel layer. Those findings could be explained by different reasons. Firstly, from a numerical point of view, wind effect on extractor is always beneficial. It is not necessary the case in a real environment due to the possible angle between wind direction and exit of the duct which can have its flow blocked. Secondly, the wind's turbulence and fluctuations can have a negative impact on air flow that is not taken into account in the calculations. Finally, results obtained with the model can be sensitive to the variation of some parameters used. Figure 4 show the impact of the variation of relevant parameters on averaged air flow from duct during the period.

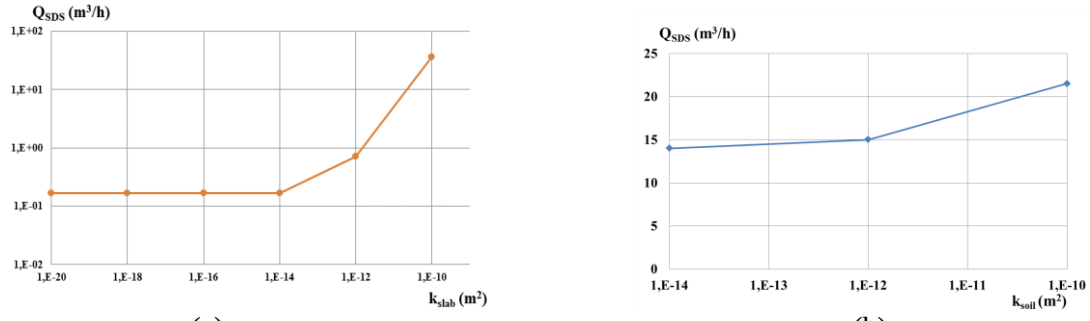

(a) (b)

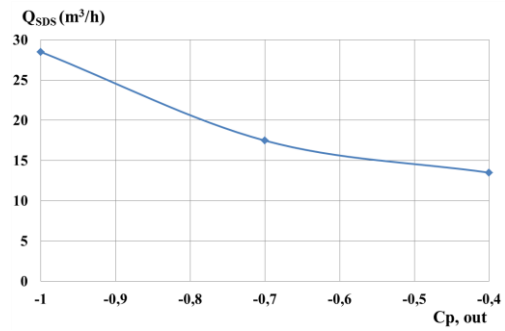

(c)

Figure 4: impact of variations of (a) slab permeability, (b) soil permeability and (c) extractor suction coefficient on averaged air flow from the SDS duct.

Despite assumptions of the model and some uncertainties due to a lack of knowledge on some relevant parameters, it can be concluded that numerical results obtained are more satisfactory compared than the experimental ones. As complementary results and with an analogy with experimental results presented in figure 1 b, figure 5 shows the percentage of running time of the system along the considered period above three thresholds. The same remarks can be made with the other numerical and experimental results.

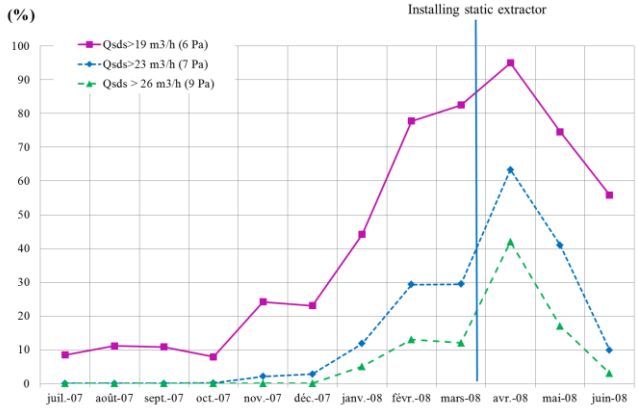

Figure 5: Percentage of running time of the system along the considered period above three thresholds.

4.2 Sensitivity study on the impact of meteorological conditions

To show the interest of this model, a sensitivity study has been conducted to analyze the impact of different meteorological conditions on mechanical running characteristics of passive SDS, for a given dwelling. Figure 6 show meteorological conditions used for this study.

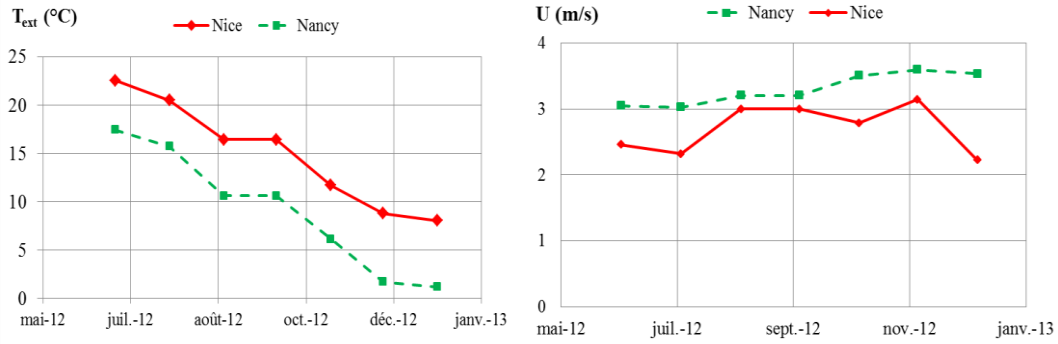

(a) (b)

Figure 6: external temperature (a) and wind velocity (b) for two different cities, Nancy and Nice, in France (monthly averaged).

It can be seen that external temperature is always lower in Nancy compared to Nice. The monthly averaged force of the wind is higher. Figure 7 presents numerical results obtained for air flow through passive SDS and for gravel depressurization along time for the two towns and during the considered period

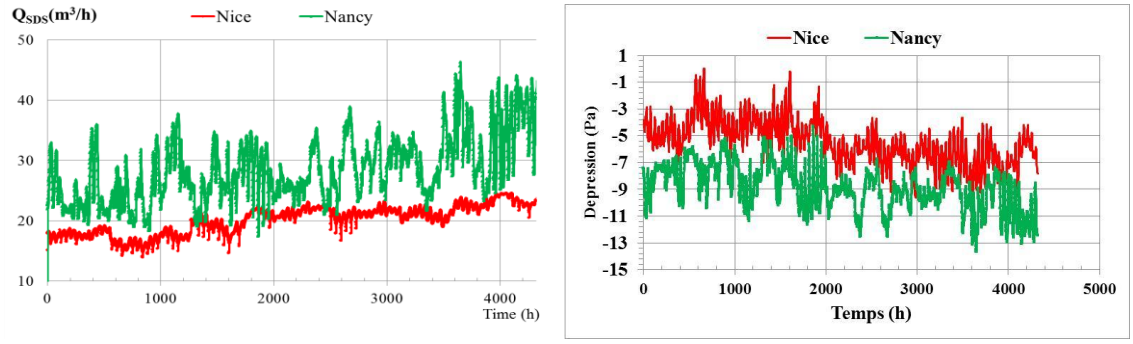

(a) (b)

Figure 7: numerical air flow through passive SDS (a) and gravel depressurization (b) for Nice and Nancy.

It can be seen that mechanical running of passive SDS is more effective in Nancy than in Nice. For the same result, figure 8 shows the percentage of running time of the system along the considered period above three thresholds for the two towns.

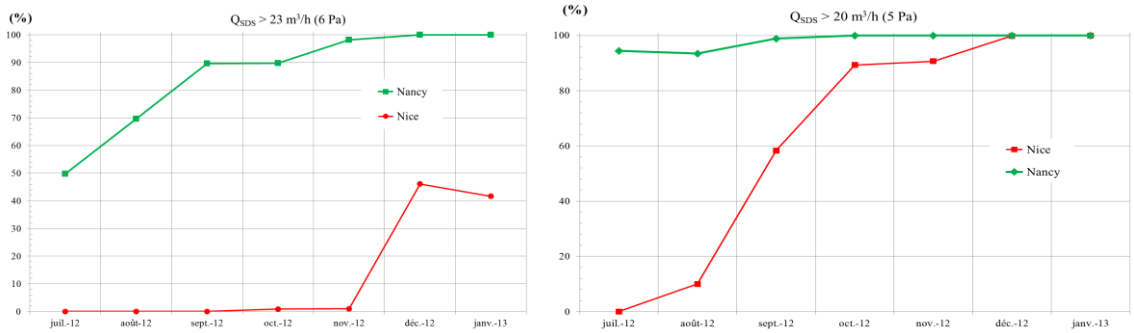

Figure 8: Percentage of running time of the system along the considered period above two thresholds for Nice and Nancy.

This figure allows us to say that for dwelling considered in these calculations, passive SDS can be more efficient if the dwelling is in Nancy region and less efficient if it is in Nice region. As shown in figure 6, the reason is that Nancy has a colder climate with wind generally slightly higher. This first sensitivity study show the potential interest of the model developed to test the ability of the passive SDS to be efficient for a considered building in given meteorological conditions. It could then be an help to dimension the system.

5 CONCLUSION

In this paper, a method based on the development of analytical air flow models to study soil gas transfer is presented to design passive Soil Depressurization System (SDS). This airflow model developed to study mechanical running of passive SDS is integrated in a multizone airflow building code. This integration allows to take into account the impact of meteorological conditions (stack effect, wind), building characteristics (height, diameter of duct for SDS, airtightness of building) and ventilation systems.

Preliminary field verification results for extracted flow using passive soil depressurization in an experimental dwelling are presented and discussed. The results obtained are quite satisfactory. Also preliminary sensitivity studies were conducted to analyze the impact of different meteorological conditions on mechanical running characteristics of passive SDS, for

a given dwelling. This study shows that the airflow model developed is accurate enough to design passive SDS systems, depending on local meteorological conditions and building characteristics.

6 ACKNOWLEDGMENT

This study was conducted in the framework of a Ph.D at CSTB (Scientific and Technical Center for Building) in collaboration with LaSIE (Laboratory of Engineering Sciences for Environment) at University of La Rochelle and partly supported by the ADEME (French Environment and Energy Management Agency).Complementary experiments needed for this study to determine soil permeability were conducted by IRSN (Institute for Radiological Protection and Nuclear Safety Institut).

Annex: Pressure loss in gravel layer

Air flow in a gravel layer can be approached by the nonlinear equation of Darcy-Forchheimer (Bonnefous, 1992):

$$\nabla P = -\frac{\mu}{k} c u^2 - \frac{\mu}{k} u \tag{A1}$$

with μ (Pa.s) the dynamic viscosity of air, k (m²) the air permeability of the gravel, c the Forchheimer coefficient and u (m/s) the velocity of air.

On this basis, we assume that the pressure difference between two interfaces in gravel layer can be written as followed:

$$P_g - P_e = a_1 Q^2 + b_1 Q \tag{A2}$$

The analogy with Darcy-Forchheimer equation (A1) implies that a_1 et b_1 coefficients are respectively proportional to à k_c/μ et k/μ.

$$a_1 = \frac{\mu}{k} c \alpha_1 \; ; \; b_1 = \frac{\mu}{k} \beta_1 \tag{A3}$$

Equation (A2) becomes:

$$P_g - P_e = \frac{\mu}{k} c \alpha_1 Q^2 + \frac{\mu}{k} \beta_1 Q \tag{A4}$$

In this equation, $\frac{\mu}{k} c \alpha_1$ and $\frac{\mu}{k} \beta_1$ need to have the dimension of a resistance (Pa.s/m^3). Using dimensional analysis, it can be concluded that:

$$\alpha_1 = \left[\frac{1}{M^3}\right] \text{and} \beta_1 = \left[\frac{1}{M}\right] \tag{A5}$$

It is assumed that a1 and b1 include a shape factor S(m),depending on geometry considered between the two interfaces. So that:

$$\alpha_1 = A_c^{-1} S^{-1} \text{and} \beta_1 = S^{-1} \tag{A6}$$

with A_c (m²) a surface depending on shape of fluid interface. Replacing eq. (A6) in eq. (A4) and considering a resistance of gravel layer as Rg = μ/(kS), eq. (A4) becomes:

$$P_g - P_e = R_g c A_c^{-1} Q^2 + R_g Q \tag{A7}$$

For model presented in this paper, it is needed to define Rg and Ac for the two configurations as presented below:

Configuration 1:

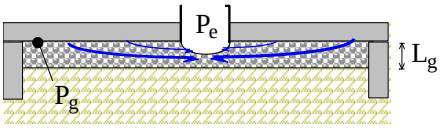

Configuration 2:

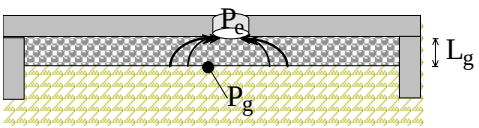

$$R_{g1} = \frac{\mu}{k}\frac{1}{\pi D} \quad ; \quad A_c = A_h = 2\pi D^2/4$$

$$R_{g2} = \frac{\frac{\mu}{k}\left[1-\left(\frac{D}{5.66L_g}\right)\right]}{1.85D} \quad ; \quad A_c = A_{duct} = \pi D^2/4$$

For configuration 1, it is based on the definition a thermal flux between a semi-infinite surface and a hemisphere (Holman, 2010), with D (m) the diameter of the hemisphere and A_h (m²) the surface of the hemisphere.

For configuration 2, it is based on the definition of thermal flux between an infinite surface and a cylinder (Sunderland and Johnson, 1964), with L_g (m), the depth of gravel layer and A_{duct} (m) the surface of cylinder entrance. Please refer to the main conclusions of the work.

7 REFERENCES

Abdelouhab M. (2011). *Contribution à l'étude du transfert des polluants gazeux entre le sol et les environnements intérieurs des bâtiments*. Thèse Université de La Rochelle.

Abdelouhab M., Collignan B. and Allard F. (2010). *Experimental study on passive Soil Depressurization System to prevent soil gaseous pollutants into building*. Building and Environment, 45, 2400-2406.

Bonnefous Y. (1992). *Étude numérique des systèmes de ventilation du sol pour diminuer la concentration en radon dans l'habitat*. Thèse de doctorat en Génie Civil : sols, matériaux, Structures et Physique du bâtiment, Institut National des Sciences Appliquées de Lyon, 256 p.

Collignan B., Abdelouhab M. Allard F., 2008. *Experimental study on passive sub-slab depressurisation system. Proceedings of the American Association of Radon Scientists and Technologists 2008*. International Symposium, September 14-17, 2008, Las Vegas USA. AARST © 2008.

Collignan B. O'Kelly P., 2003. *Dimensioning of soil depressurisation system for radon remediation in existing building.* Proceedings of Healthy Building conference, 7th- 11th Dec. 2003, Singapore, 517-523.

Collignan B., O'Kelly P. Pilch E., 2004. *Basement depressurisation using dwelling mechanical ventilation system.* 4th European Conference on Protection against radon at home and at work, 28th June- 2nd July 2004 Praha, Czech republic.

Cripps A.J. (1998). *Air Modeling and measurement of soil gas flow*. AIVC 11619, Construction Research communication Ltd.

Diallo T.M.O., Collignan B., Allard F. (2012), *Analytical quantification of airflows from soil through building substructures*, 10.1007/s12273-012-0095-2,2012. Building Simulation Journal.

Elenbaas W. (1942). *Heat Dissipation of Parallel Plates by Free Convection*,Physica, Vol. IX, No.1, p.1–28.

Gadgil A.J., Bonnefous Y.C., Fisk W.J. *Relative effectiveness of Sub-Slab Pressurization and Depressurization Systems for Indoor Radon Mitigation: Studies with an Experimentally Verified Numerical Model*. In: Proceedings of the 1992 international symposium on Radon

Gray A., Read S., McGale P. Darby, S., 2009. *Lung cancer deaths from indoor radon and the cost effectiveness and potential of policies to reduce them.* Brit Med J. 338, 3110-3121.

Holford, D.J. & Freeman, H.D. (1996) *Effectiveness of a Passive Subslab Ventilation Systemn in Reducing Radon Concentrations in a Home.* Environ. Sci. Technol. 30, 2914-2920.

Holman J. P. (2010). *Heat Transfer*, 10th Edition, Jack P. Holman, Southern Methodist University McGraw-Hill, New York, 2010. ISBN-13 9780073529363

I.E IDEL'CIK, (1969). *Memento des pertes de charge – Coefficients de pertes de charge singulières et de pertes de charge par frottement*. Traduction du Russe par Madame M. Meury. Collection n°13 du Centre de Recherches et d'essais du Chatou. Eyrolles, Paris.

IRSN, (2012). *Mesure de la perméabilité effective du sol aux gaz autour de la maison expérimentale MARIA du CSTB*. RT/PRP-DGE/2012-00019.

Koffi J. (2009) *Analyse multicritère des stratégies de ventilation en maisons individuelles*. Thèse Université de la Rochelle.

Mounajed, M.R., (1989). *La modélisation des transferts d'air dans les bâtiments application â l'étude de la ventilatio*n. PhD thèse. L'École Nationale des Ponts et Chaussées.

Sunderland J. E., Kenneth R.J. (1964). *Shape factors for heat conduction through bodies with isothermal or convective boundary conditions*. ASHRAE 71st Annual Meeting in Cleveland, Ohio.

Turk B.H., Harrison J.and Sextro R. G. (1991). *Performance of radon control systems. Energy and Buildings*.Vol.17, pp. 157-175.

USEPA, 1993. *Radon reduction techniques for existing detached houses. Technical guidance (third edition) for Active Soil Depressurization systems*. EPA/625/R-93/011.